



## High performance of solvothermally prepared VO<sub>2</sub>(B) as an anode for aqueous rechargeable lithium batteries

SANJA MILOŠEVIĆ<sup>1</sup>, IVANA STOJKOVIĆ<sup>2</sup>, MIODRAG MITRIĆ<sup>3</sup>  
and NIKOLA CVJETIĆANIN<sup>2\*</sup>

<sup>1</sup>The Vinča Institute, Department of Materials Science, University of Belgrade, P. O. Box 522, 11001 Belgrade, Serbia, <sup>2</sup>Faculty of Physical Chemistry, University of Belgrade, 11158 Belgrade, Serbia and <sup>3</sup>The Vinča Institute, Laboratory for Theoretical and Condensed Matter Physics, University of Belgrade, P. O. Box 522, 11001 Belgrade, Serbia

(Received 22 September, revised 3 December, accepted 25 December 2014)

**Abstract:** The VO<sub>2</sub>(B) was synthesized via a simple solvothermal route at 160 °C in ethanol. The initial discharge capacity of the VO<sub>2</sub>(B) anode, in saturated aqueous solution of LiNO<sub>3</sub>, was 177 mAh g<sup>-1</sup> at a current rate of 50 mA g<sup>-1</sup>. After 50 cycles, the capacity fade was 4 %, but from 20<sup>th</sup>–50<sup>th</sup> cycle, no capacity drop was observed. The VO<sub>2</sub>(B) showed very good cyclability at a current rate of even 1000 mA g<sup>-1</sup> with initial discharge capacity of 92 mAh g<sup>-1</sup>. The excellent electrochemical performance of VO<sub>2</sub>(B) was attributed to the stability of micro–nano structures to a repeated intercalation/deintercalation process, very good electronic conductivity as well as the very low charge transfer resistance in an aqueous electrolyte.

**Keywords:** aqueous rechargeable lithium batteries; anode materials; discharge capacity; electrochemical impedance spectroscopy; electric conductivity.

### INTRODUCTION

Most of the present lithium technology is based on organic electrolytes.<sup>1</sup> The most common of these electrolytes are expensive, toxic and flammable liquids that may cause accidents in the case of improper use.<sup>1,2</sup> One way to overcome the safety issue is to use aqueous electrolytes which are environmentally benign. The assembly of aqueous lithium batteries is simpler and cheaper than for their organic counterparts because it does not demand the usage of argon-filled chambers in which moisture and oxygen have to be excluded. Unfortunately, aqueous rechargeable lithium batteries (ARLBs) cannot deliver a high voltage, because their voltage is restricted by the potentials of the evolution of hydrogen and oxygen. However, aqueous electrolytes have conductivities which are

\*Corresponding author. E-mail: nikola.cvj@ffh.bg.ac.rs  
doi: 10.2298/JSC140922128M

typically two orders of magnitude higher than that of organic systems, which enables the achievement of a high rate capability. From the time when the first papers were published in 1994/5 by Dahn's group,<sup>3–5</sup> interest in ARLBs increased. Numerous intercalation compounds have been tested in alkaline and neutral aqueous electrolytes,<sup>5–12</sup> especially in the last five years.<sup>12–21</sup> Among them, the vanadium oxide family of compounds has attracted much attention as anodic materials for ARLBs. Due to a suitable electrode potential and tunnel structure, VO<sub>2</sub>(B), one of the polymorphs of VO<sub>2</sub>, was already used as the anodic material in the first ARLBs.<sup>3,5</sup> However, this compound was neglected in subsequent researches compared to other vanadium oxides. Transformation from bulk to nano-dimensions brought new qualities to electrode materials, such as larger surface area, shorter diffusion lengths of Li-ion, capability for buffering large volume changes and possible new storage mechanisms, leading to higher specific capacity, faster kinetics and enhanced cycle life.<sup>1,22</sup> This has increased the interest for VO<sub>2</sub>(B) both as a cathodic and anodic material for organic and aqueous electrolytes based lithium batteries, respectively. In recent years VO<sub>2</sub>(B) has been synthesized with different micro/nano-morphologies: nanowire arrays,<sup>23</sup> networks of nanofilaments,<sup>24</sup> nanobelts and nanosheets,<sup>25–28</sup> nanorods,<sup>29,30</sup> ultra-thin nanowires,<sup>31</sup> flower-like micro–nano structures,<sup>13</sup> and hollow micro-spheres with a nanothorn surface.<sup>32</sup> The majority of these morphologies have been synthesised by more or less sophisticated hydrothermal/solvothermal methods.

In this paper, the high capacity and excellent galvanostatic cyclic behaviour of solvothermally prepared VO<sub>2</sub>(B), in saturated aqueous LiNO<sub>3</sub> solution and up to current rates of 1000 mA·g<sup>-1</sup>, is primarily demonstrated.

## EXPERIMENTAL

Nanostructured VO<sub>2</sub>(B) was synthesized *via* a simple one-step solvothermal (ST) process that was published recently.<sup>33</sup> Thus, without using any additives or surfactants, a mixture of vanadium pentoxide (Merck 99.99 %) and ethanol (Merck 96 %) was treated in a Teflon-lined stainless-steel autoclave at 160 °C for 24 h. The obtained blue–black powder was rinsed several times with ethanol and then dried at 50 °C.

LiCr<sub>0.15</sub>Mn<sub>1.85</sub>O<sub>4</sub>, as the counter electrode (cathode) material for a two electrode cell, was prepared by the glycine–nitrate method (GNM).<sup>34</sup>

The characterization of VO<sub>2</sub>(B) and LiCr<sub>0.15</sub>Mn<sub>1.85</sub>O<sub>4</sub> by X-ray diffraction (XRD) was presented in previous papers.<sup>33,34</sup> The morphological characterization of VO<sub>2</sub>(B) was performed on a JEOL JSM-6390 LV scanning electron microscope (SEM). The SEM images of LiCr<sub>0.15</sub>Mn<sub>1.85</sub>O<sub>4</sub> corresponded to those published previously<sup>34</sup> and are not presented here.

The preparation of electrodes from both materials was performed in the same way. The active material, carbon black and poly(vinylidene fluoride) in weight ratio 85:10:5 were homogeneously mixed in *N*-methyl 2-pyrrolidone. The slurry was treated for about 30 min in an ultrasonic bath, deposited on the stainless steel (SS) discs electrodes ( $\approx$ 6.2 cm<sup>2</sup>) and Pt foil (2 cm<sup>2</sup>), and dried under vacuum at 120–140 °C for at least 4 h.

Galvanostatic charging/discharging measurements were performed using a software-controlled Arbin BT-2042 device, in a two-electrode arrangement within the voltage range 0.5–1.65 V. The electrode materials applied to the SS discs were mounted in the body of a cell made from Plexiglas. The electrodes were separated with eight filter paper sheets (total thickness  $\approx$  1 mm) soaked in saturated aqueous solution of LiNO<sub>3</sub> as the electrolyte. The capacity calculations were based on the weight of the active anode material, *i.e.*, VO<sub>2</sub>(B).

For electrical conductivity measurements, VO<sub>2</sub>(B) powder was pressed into a pellet, 8 mm in diameter and 1.835 mm thick. Good electrical contact was realized by coating silver paste onto both contact surfaces of the pellet. The conductivity was measured by means of a Wayne Kerr B224 AC bridge at a fixed frequency of 1 kHz. The self-made two electrode conductometric cell for solid conductors was placed inside a small cylindrical oven, heated up to 120 °C, and the measurements were performed in the cooling regime.

Electrochemical impedance spectroscopy (EIS) measurements were performed in a three electrode cell (VO<sub>2</sub>(B) deposited on Pt foil – working electrode, Pt foil – counter electrode, SCE – reference electrode) filled with a saturated aqueous solution of LiNO<sub>3</sub> using a Gamry PCI4/300 Potentiostat/Galvanostat. An AC amplitude of 5 mV was applied in the frequency range 100 kHz–0.1 Hz. The programme EIS Spectrum Analyzer, version 1.0, was used for fitting data to the equivalent circuit model.

## RESULTS AND DISCUSSION

SEM images of VO<sub>2</sub>(B) synthesized solvothermally are shown in Fig. 1. The product consisted of different nano-units, such as single nanoparticles, rods and flat particles, mutually welded in different irregularly shaped micrometre-sized structures, Fig. 1A. The shape of micro–nano structures mainly resembled those previously described in more detail.<sup>33</sup> Additionally, some amount of large spherical micrometre-sized particles, the surfaces of which were covered with mostly spherical particles of size mainly below 300 nm, was also observed, Fig. 1B.

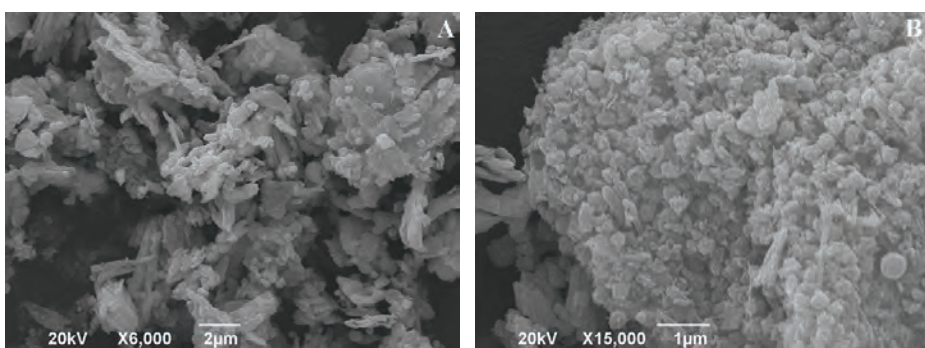


Fig. 1. SEM micrograph of VO<sub>2</sub>(B): A) irregularly shaped particles composed from welded nano-units; B) large spherical VO<sub>2</sub>(B) particles covered with spherical nano particles.

The voltage range, 0.5–1.65 V, for the galvanostatic charge/discharge experiments was determined based on the electrochemical performance of both VO<sub>2</sub>(B) and LiCr<sub>0.15</sub>Mn<sub>1.85</sub>O<sub>4</sub> in saturated aqueous solution of LiNO<sub>3</sub>, per-

ceived by cyclic voltammetry.<sup>33,34</sup> Here, LiCr<sub>0.15</sub>Mn<sub>1.85</sub>O<sub>4</sub> was used as cathodic material instead of most commonly used LiMn<sub>2</sub>O<sub>4</sub>, because the substitution of some manganese with Cr<sup>3+</sup> gives a faster cathode in saturated aqueous solution of LiNO<sub>3</sub>.<sup>34</sup> A two-fold stoichiometric excess of the cathode material LiCr<sub>0.15</sub>Mn<sub>1.85</sub>O<sub>4</sub> was used in order to avoid the cathode limiting the cell performance.

Although there was no voltage plateau during discharging (Figs. S-1 and S-2 of the Supplementary material to this paper), the discharge capacity of the VO<sub>2</sub>(B) anode was very high and exceptionally stable, Fig. 2. In the first 50 cycles, the VO<sub>2</sub>(B) anode was tested with a constant current of 50 mA g<sup>-1</sup>, Fig. 2A, and then every next ten cycles the current was increased to 100, 150, 200, 500 and 1000 mA g<sup>-1</sup>, Fig. 2B. The initial discharge capacity was 177 mAh g<sup>-1</sup> at current rate 50 mA g<sup>-1</sup>. The discharge capacity then increased to 182 mAh g<sup>-1</sup>, and after the 5<sup>th</sup> cycle, started to decrease. After twenty cycles, the discharge capacity became constant at 170 mAh g<sup>-1</sup>. The capacity fade after 50 cycles was only 4 %. The obtained value of the capacity exceeded the theoretical capacity of Li<sub>0.5</sub>VO<sub>2</sub>(B) (161.6 mAh g<sup>-1</sup>). This could mean that surface storage participates in the overall charge storage. Figure 2B shows that VO<sub>2</sub>(B) had a quite high

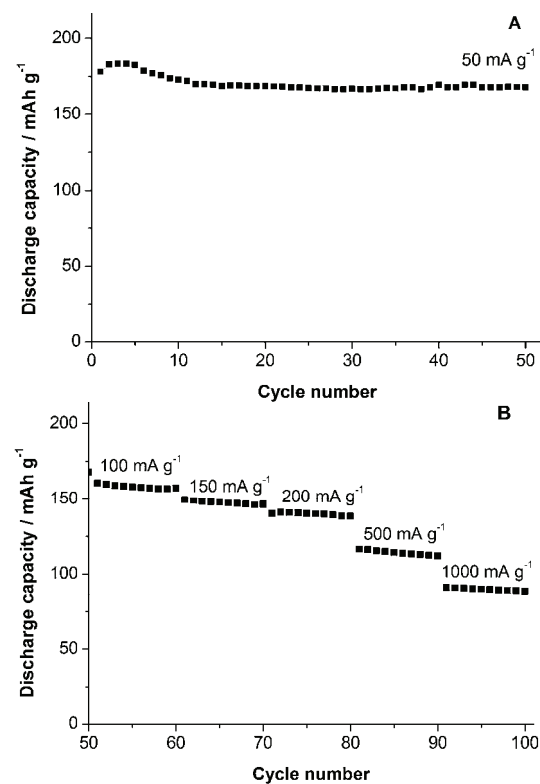


Fig. 2. Discharge capacity of VO<sub>2</sub>(B) anode in a saturated aqueous solution of LiNO<sub>3</sub>: A) at a current rate of 50 mA g<sup>-1</sup> and B) at different current rates: 100, 150, 200, 500 and 1000 mA g<sup>-1</sup>.

discharge capacity and retained very good cycling stability when the current rates were significantly increased. The initial discharge capacities were 161, 149, 140, 117 and 92 mAh g<sup>-1</sup> at current rates 100, 150, 200, 500 and 1000 mA g<sup>-1</sup>, respectively. The capacity fade after ten cycles was below 4 % in all cases. These are much better characteristics in comparison to other intercalation anode materials hitherto tested in aqueous electrolytes with similar current rates.<sup>12–14,16,17,19</sup> Recently, Tang *et al.* published that a hybrid of V<sub>2</sub>O<sub>5</sub> and MWCNTs coated with polypyrrole as anode for ARLB had excellent cycling performance, but its reversible capacity was only 60 mAh g<sup>-1</sup> at 200 mA g<sup>-1</sup>.<sup>20</sup>

The Nyquist plot of the lithiated VO<sub>2</sub>(B) (Li<sub>0.5</sub>VO<sub>2</sub>) electrode showed one depressed semicircle in the high-to-medium frequency region, which could be assigned to charge-transfer resistance ( $R_{ct}$ ), and a near unity-slope line at lower frequencies, which could be considered as Warburg impedance, Fig. 3A. The data were successfully fitted in the frequency range 100 kHz–1 Hz to the equivalent circuit model shown in the inset of Fig. 3A. The charge transfer resistance amounted to only 1.8 Ω, which is six times and an order of magnitude smaller than for NiO–LiV<sub>3</sub>O<sub>8</sub> and LiV<sub>3</sub>O<sub>8</sub> electrode, respectively, in the same

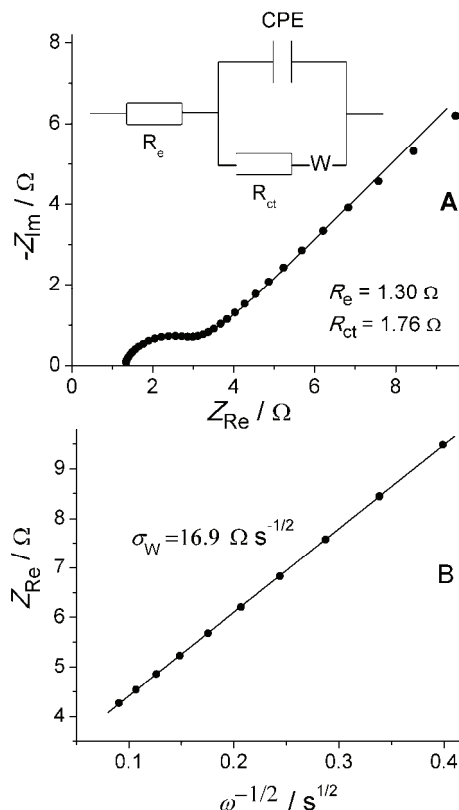


Fig. 3. EIS data of lithiated VO<sub>2</sub>(B) electrode: A) Nyquist plot and the equivalent circuit used to fit the impedance data ( $R_e$  – resistance of electrolyte,  $R_{ct}$  – charge transfer resistance, CPE – constant phase element, W – Warburg impedance) and B) the  $Z'$  vs.  $\omega^{-1/2}$  plot used for determination of  $D_{Li^+}$ . ● represents data, line represents fit.

aqueous electrolyte.<sup>19</sup> The calculated value of  $R_{ct}$  was also approximately two orders of magnitude smaller than those obtained for similar anodes in some organic electrolytes.<sup>35,36</sup> The diffusion coefficient of the lithium ion was calculated from the equation:<sup>37,19</sup>

$$D = \frac{R^2 T^2}{2A^2 n^4 F^4 c_{\text{Li}^+}^2 \sigma_W^2} \quad (1)$$

where  $\sigma_W$  is the Warburg coefficient, and according to the equation:<sup>37</sup>

$$Z_{R_e} = R_e + R_{ct} + \sigma_W \omega^{-1/2} \quad (2)$$

which is valid in the low-frequency region. Equation (2) represents the slope of the  $Z_{R_e}$  vs.  $\omega^{-1/2}$  plot, Fig. 3B. The concentration of  $\text{Li}^+$  in  $\text{Li}_{0.5}\text{VO}_2$  was obtained using unit cell parameters of this monoclinic compound:  $a = 12.03 \text{ \AA}$ ,  $b = 4.0 \text{ \AA}$ ,  $c = 6.42 \text{ \AA}$  and  $\beta = 106.6^\circ$ ,<sup>38</sup> bearing in mind that the unit cell contains eight formula-units. The crystal structure of  $\text{Li}_{0.5}\text{VO}_2$  is very similar to the parent  $\text{VO}_2(\text{B})$ , which is monoclinic (space group C12/m1 – ICSID 73855), having the unit cell 9.2 % elongated in the  $b$ -axis direction.<sup>38</sup> By taking  $R = 8.314 \text{ J} \cdot \text{mol}^{-1} \text{ K}^{-1}$ ,  $T = 298 \text{ K}$ ,  $A = 2 \text{ cm}^2$ ,  $n = 0.5$ ,  $F = 96485 \text{ C mol}^{-1}$ ,  $c_{\text{Li}^+} = 0.0224 \text{ mol} \cdot \text{cm}^{-3}$  and  $\sigma_W = 16.9 \Omega \text{ s}^{-1/2}$ , the calculated value of the diffusion coefficient is equal to  $D_{\text{Li}^+} = 1 \times 10^{-12} \text{ cm}^2 \text{ s}^{-1}$ . This value is almost the same as the diffusion coefficient of  $\text{Li}^+$  ( $1.69 \times 10^{-12} \text{ cm}^2 \text{ s}^{-1}$ ) in  $\text{LiV}_3\text{O}_8$ ,<sup>19</sup> determined by the same method, but is much smaller than the diffusion coefficients of  $\text{Li}^+$  in carbon-coated  $\text{VO}_2(\text{B})$  nanobelts ( $2.6 \times 10^{-10}$ – $8.6 \times 10^{-10} \text{ cm}^2 \text{ s}^{-1}$ ), obtained from cyclic voltammetry experiments in an organic electrolyte.<sup>36</sup>

High power devices demand fast transport of electrons, therefore the electronic conductivities of cathode and anode materials for LBs is of very great importance.  $\text{VO}_2(\text{B})$  is a semiconductor, but there is not much data about its electronic conductivity.<sup>39,40</sup> The temperature dependence of the specific conductivity of the  $\text{VO}_2(\text{B})$  synthesised in this work is shown in Fig. 4. From this almost ideally linear, logarithmic-type plot, the activation energy for electric conductivity was determined to be  $21.5 \text{ kJ} \cdot \text{mol}^{-1}$  or  $0.223 \text{ eV}$ . The room temperature electric conductivity is  $4.7 \times 10^{-3} \text{ S cm}^{-1}$ , which is in good agreement with the value ( $\approx 1 \times 10^{-2} \text{ S cm}^{-1}$ ) obtained by Corr. *et al.*<sup>40</sup> for  $\text{VO}_2(\text{B})$  nanorods, pressed into a pellet, by four-probe resistivity measurements. This value is several orders of magnitude higher than those of some anode and cathode materials for lithium batteries, such as  $\text{Li}_4\text{Ti}_5\text{O}_{12}$  ( $3.5 \times 10^{-8} \text{ S cm}^{-1}$ )<sup>41</sup> and  $\text{LiFePO}_4$  ( $10^{-9}$ – $10^{-10} \text{ S cm}^{-1}$ ).<sup>42</sup>

It was shown recently that electrochemical cycling stability of some cathode<sup>43,44</sup> and anode<sup>45</sup> materials for ARLBs, mostly layer-structured compounds, abruptly decreases in the low-pH solutions due to the co-intercalation of  $\text{H}^+$  ions. Such behaviour was not observed in this study, despite the low pH

(around 3.2) of the saturated ( $\approx 9$  M) aqueous solution of LiNO<sub>3</sub>. The tunnel-structured VO<sub>2</sub>(B) and the spinel-structured LiCr<sub>0.15</sub>Mn<sub>1.85</sub>O<sub>4</sub> used as the cathode are not, most probably, energetically favourable for the accommodation of H<sup>+</sup> ions. This was already confirmed, at least to some extent, for spinel-type compounds.<sup>44</sup>

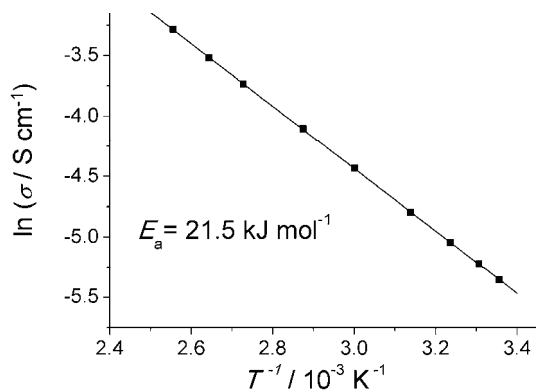


Fig. 4. Temperature dependence of the specific conductivity of VO<sub>2</sub>(B). ● represents data, line represents fit.

Nanostructures of VO<sub>2</sub>(B), such as nanobelts, nanorods and nanosheets, can offer a high initial capacity due to their large surface area and the short diffusion length of Li-ion. Unfortunately these nanostructures mostly suffer from significant capacity fade. Such a loss of capacity, on the one hand, is due to pulverization of the electroactive material during cycling, resulting in the loss of some amount of active mass. On the other hand, nano-sized materials have a large surface area and high surface energy that favour the formation of agglomerates and leads to the loss of the insertion capacity of Li<sup>+</sup>.<sup>35,46</sup> It was already documented that 3D VO<sub>2</sub>(B) structures such as micro/nano-flowers<sup>13</sup> and hollow micro-spheres<sup>32</sup> show improved electrochemical characteristics because they have collective properties from the self-assembling of nano-units into micrometre-sized structures. The VO<sub>2</sub>(B) obtained in this study enabled the excellent performance of the ARLB, most likely due to both the micro–nano morphology and the use of a water-based electrolyte. Although the nano-units were mutually welded in irregularly shaped microstructures, they were robust enough on exposure to the aqueous electrolyte to give a stable intercalation capacity of lithium ions. These micro–nano structures also had very good electronic conductivity, but the rate of diffusion of Li<sup>+</sup> inside these structures, although one of the most important properties, seems not to have been a prevailing factor for the excellent electrochemical performance. The EIS data indicated that not only the high conductivity of aqueous electrolyte, but also the very low charge transfer resistance and the absence of resistive surface film seems to be responsible for the very fast insertion/extraction of lithium ions.

All the presented electrochemical experiments were performed in aerated aqueous solution, without testing the oxygen content. The elimination of dissolved oxygen may significantly improve the performance of some ARLBs.<sup>47</sup> However, in the presence of oxygen, carbon coating of the cathode may exceptionally improve the rate capability and cycle life, as was recently demonstrated for a VO<sub>2</sub>(B)/LiNO<sub>3</sub>(sat)/LiFe<sub>1-x</sub>V<sub>x</sub>PO<sub>4</sub>-C aqueous battery.<sup>48</sup> The precise influence of dissolved oxygen on VO<sub>2</sub>(B) anodes in saturated aqueous solutions of LiNO<sub>3</sub> remains to be examined in the near future.

#### CONCLUSIONS

The VO<sub>2</sub>(B) was synthesised by a simple, low-cost and environmentally friendly solvothermal method. It displayed exceptional characteristics during galvanostatic cycling: the initial discharge capacity was 177, 161, 149, 140, 117 and 92 mAh g<sup>-1</sup> at current rates 50, 100, 150, 200, 500 and 1000 mA g<sup>-1</sup>, respectively, with a very small capacity fade. The obtained material showed very high electronic conductivity and moderately fast diffusion of lithium ions. The robust micro–nano structures of VO<sub>2</sub>(B) in contact with the highly conductive aqueous electrolyte formed an electrode/electrolyte interface with fast charge transfer kinetics, which enabled the excellent rate performance of the anode. Further improvement of hydrothermal/solvothermal synthetic methods in obtaining strong micro–nano structures, in the first place more uniform in shape, may offer superior electrode materials for aqueous rechargeable lithium batteries.

#### SUPPLEMENTARY MATERIAL

Charge/discharge curves of a VO<sub>2</sub>(B) anode are available electronically from <http://www.shd.org.rs/JSCS/>, or from the corresponding author on request.

*Acknowledgements.* This work was supported by the Ministry of Education, Science and Technological Development of the Republic of Serbia (Contract No. III45014).

ИЗВОД

ВИСОКЕ ПЕРФОРМАНСЕ СОЛВОТЕРМАЛНО СИНТЕТИСАНОГ VO<sub>2</sub>(B) КАО АНОДНОГ МАТЕРИЈАЛА ЗА СЕКУНДАРНЕ ЛИТИЈУМСКЕ БАТЕРИЈЕ СА ВОДЕНИМ ЕЛЕКТРОЛИТОМ

САЊА МИЛОШЕВИЋ<sup>1</sup>, ИВАНА СТОЈКОВИЋ<sup>2</sup>, МИОДРАГ МИТРИЋ<sup>3</sup> И НИКОЛА ЦВЈЕТИЋАНИН<sup>2</sup>

<sup>1</sup>Инситијуј Винча, Лабораторија за материјале, Универзитет у Београду, Ј. Ђорђевића 522, 11001 Београд,

<sup>2</sup>Факултет за физичку хемију, Универзитет у Београду, 11158 Београд 118 и <sup>3</sup>Инситијуј Винча,

Лабораторија за шеријску физику и физику кондензоване материје, Универзитет у Београду,

Ј. Ђорђевића 522, 11001 Београд

VO<sub>2</sub>(B) је синтетисан једноставним солвотермалним поступком на 160 °C у етапу. Тестиран је као анодни материјал за секундарне литијумске батерије у засићеном раствору литијум-нитрата методом галваностатског пунења и пражњења. При специфичним јачинама струје од 50 до 1000 mA g<sup>-1</sup> VO<sub>2</sub>(B) је показао висок почетни капацитет при пражњењу од 177 до 92 mAh g<sup>-1</sup>, уз веома мали пад капацитета. Високе перформансе овог материјала потичу од стабилности робусних микро–нано структура

према великим броју интеркалација/деинтеркалација јона литијума као и од добре електронске проводљивости и малог отпора преносу наелектрисања.

(Примљено 22. септембра, ревидирано 3. децембра, прихваћено 25. децембра 2014)

#### REFERENCES

1. B. Scrosati, J. Garche, *J. Power Sources* **195** (2010) 2419
2. D. Wainwright, *Mat. Tech.* **11** (1996) 9
3. W. Li, J. R. Dahn, D. Wainwright, *Science* **264** (1994) 1115
4. W. Li, W. R. McKinnon, J. R. Dahn, *J. Electrochem. Soc.* **141** (1994) 2310
5. W. Li, J. R. Dahn, *J. Electrochem. Soc.* **142** (1995) 1742
6. G. X. Wang, S. Zhong, D. H. Bradhurst, S. H. Dou, H. K. Liu, *J. Power Sources* **74** (1998) 198
7. J. Kohler, H. Makahira, H. Uegaito, H. Inoue, M. Toki, *Electrochim. Acta* **46** (2000) 59
8. Y. Wang, Y. Xia, *Electrochim. Commun.* **7** (2005) 1138
9. G. J. Wang, H. P. Zhang, L. J. Fu, B. Wang, Y. P. Wu, *Electrochim. Commun.* **9** (2007) 1873
10. G. J. Wang, N. H. Zhao, L. C. Yang, Y. P. Wu, H. Q. Wu, R. Holze, *Electrochim. Acta* **52** (2007) 4911
11. G. J. Wang, L. J. B. Wang, N. H. Zhao, Y. P. Wu, R. Holze, *J. Appl. Electrochem.* **38** (2008) 579
12. C. Z. Wu, Z. P. Hu, W. Wang, M. Zhang, J. L. Yang, Y. Xie, *Chem. Commun.* (2008) 3891
13. S. Zhang, Y. Li, C. Wu, F. Zheng, Y. Xie, *J. Phys. Chem. C* **113** (2009) 15058
14. I. Stojković, N. Cvjetićanin, I. Pašti, M. Mitrić, S. Mentus, *Electrochim. Commun.* **11** (2009) 1512
15. X.-H. Liu, T. Saito, T. Doi, S. Okada, J. Yamaki, *J. Power Sources* **189** (2009) 706
16. I. Stojković, N. Cvjetićanin, M. Mitrić, S. Mentus, *Electrochim. Acta* **56** (2011) 6469
17. M. Zhao, Q. Zheng, F. Wang, W. Dai, X. Song, *Electrochim. Acta* **56** (2011) 3781
18. H. Heli, H. Yadegari, A. Jabbari, *Mat. Chem. Phys.* **126** (2011) 476
19. L. Liu, M. Zhou, X. Wang, F. Tian, H. Guo, B. Shen, T. Hu, *J. Electrochem. Soc.* **159** (2012) A1230
20. W. Tang, X. Gao, Y. Zhu, Y. Yue, Y. Shi, Y. Wu, K. Zhu, *J. Mater. Chem.* **22** (2012) 20143
21. V. S. Nair, Y. L. Cheah, S. Madhavi, *J. Electrochem. Soc.* **161** (2014) A256
22. C. K. Chan, H. Peng, R. D. Tweten, K. Jarausch, X. F. Zhang, Y. Cui, *Nano Lett.* **7** (2007) 490
23. X. Chen, X. Wang, Z. Wang, J. Wan, J. Liu, Y. T. Qian, *Nanotechnology* **15** (2004) 1685
24. E. Baudrin, G. Sudant, D. Larcher, B. Dunn, J.-M. Tarascon, *Chem. Mater.* **18** (2006) 4369
25. G. Li, K. Chao, H. Peng, K. Chen, Z. Zhang, *Inorg. Chem.* **46** (2007) 5787
26. F. Sediri, N. Gharbi, *Mater. Lett.* **63** (2009) 15
27. J. Li, Z. Su, B. Yang, S. Cai, Z. Dong, J. Ma, R. Li, *J. Phys. Chem. Solids* **71** (2010) 407
28. G. Zakharova, I. Hellmann, V. Volkov, C. Taschner, A. Bachmatiuk, A. Leonhardt, R. Klingeler, B. Büchner, *Mater. Res. Bull.* **45** (2010) 1118
29. Ch. V. Subba Reddy, E. H. Walker Jr., S. A. Wicker Sr., Q. L. Williams, R. R. Kalluru, *Curr. Appl. Phys.* **9** (2009) 1195
30. F. J. Quites, H. O. Pastore, *Mater. Res. Bull.* **45** (2010) 892
31. G. Armstrong, J. Canales, A. R. Armstrong, P. Bruce, *J. Power Sources* **178** (2008) 723

32. H. Liu, Y. Wang, K. Wang, E. Hosono, H. Zhou, *J. Mater. Chem.* **19** (2009) 2835
33. S. Milošević, I. Stojković, S. Kurko, J. Grbović-Novaković, N. Cvjetićanin, *Ceram. Int.* **38** (2012) 2313
34. N. Cvjetićanin, I. Stojković, M. Mitić, S. Mentus, *J. Power Sources* **174** (2007) 1117
35. M. M. Rahman, J.-Z. Wang, N. H. Idris, Z. Chen, H. Liu, *Electrochim. Acta* **56** (2010) 693
36. X. Rui, D. Sim, C. Xu, W. Liu, H. Tan, K. Wong, H. H. Hng, T. M. Lim, Q. Yan, *RSC Adv.* **2** (2012) 1174
37. A. J. Bard, L. R. Faulkner, *Electrochemical methods: Fundamentals and applications*, 2<sup>nd</sup> ed., Wiley, New York, 2001, p. 383
38. P. A. Christian, F. J. Di Salvo Jr., D. W. Murphy, US Patent 4228226 (1980)
39. J. Liu, Q. Li, T. Wang, D. Yu, Y. Li, *Angew. Chem. Int. Ed.* **43** (2004) 5048
40. S. A. Corr, M. Grossman, Y. Shi, K. R. Heier, G. D. Stucky, R. Seshadri, *J. Mater. Chem.* **19** (2009) 4362
41. M. Vujković, I. Stojković, M. Mitić, S. Mentus, N. Cvjetićanin, *Mater. Res. Bull.* **48** (2013) 218
42. S.-Y. Chung, J. T. Bloking, Y.-M. Chiang, *Nat. Mater.* **1** (2002) 123
43. X. Gu, J.-L. Liu, J.-H. Yang, H.-J. Xiang, X.-G. Gong, Y.-Y. Xia, *J. Phys. Chem. C* **115** (2011) 12672
44. Q. Shu, L. Chen, Y. Xia, X. Gong, X. Gu, *J. Phys. Chem., C* **117** (2013) 6929
45. L. Bai, J. Zhu, X. Zhang, Y. Xie, *J. Mater. Chem.* **22** (2012) 16957
46. J. Huang, X. Wang, J. Liu, X. Sun, L. Wang X. Xe, *Int. J. Electrochem. Sci.* **6** (2011) 1709
47. J.-Y. Luo, W.-J. Cui, P. He, Y.-Y. Xia, *Nat. Chem.* **2** (2010) 760
48. M. Vujković, D. Jugović, M. Mitić, I. Stojković, N. Cvjetićanin, S. Mentus, *Electrochim. Acta* **109** (2013) 835.